Namani Rakesh, Sanchari Banerjee, Senthilkumar Subramaniam* and Natarajan Babu

A simplified method for fault detection and identification of mismatch modules and strings in a grid-tied solar photovoltaic system

https://doi.org/10.1515/ijeeps-2020-0001
Received January 2, 2020; accepted July 9, 2020; published online August 10, 2020

Abstract: The foremost problem facing by the photovoltaic (PV) system is to identify the faults and partial shade conditions. Further, the power loss can be avoided by knowing the number of faulty modules and strings. Hence, to attend these problems, a new method is proposed to differentiate the faults and partially shaded conditions along with the number of mismatch modules and strings for a dynamic change in irradiation. The proposed method has developed in two main steps based on a simple observation from the Current versus Voltage (I-V) characteristic curve of PV array at Line-Line (LL) fault. First, the type of fault is detected using defined variables, which are continuously updated from PV array voltage, current, and irradiation. Second, it gives the number of mismatch modules (or short-circuited bypass diodes) and mismatch strings (or open-circuited blocking diodes) by comparing with the theoretical predictions from the I-V characteristic curve of PV array. The proposed algorithm has been validated both on experimentation using small scale grid-connected PV array developed in the laboratory as well as MATLAB/Simulink simulations. Further, the comparative assessment with existing methods is presented with various performance indices to show the effectiveness of the proposed algorithm.

Keywords: line-line faults; partial shaded conditions; PV systems; short-circuited modules and stings.

1 Introduction

The generation of power in a photovoltaic (PV) system depends on the condition of the PV arrays and wiring connections, environmental conditions of site such as temperature and availability of solar radiation, and failures or faults that may occur during its operation [1]. The PV systems can be classified as PV array faults, faults in power converters and faults in interconnections of utility grid based on the location of faults. The identification of faults in PV arrays is difficult and have catastrophic effects in the entire system as explained in [2–4]. The PV array faults such as open-circuit faults, Line-Line (LL) faults, Line-Ground (LG) faults, arc faults and mismatch faults causes significant power loss in the PV system. The installations of PV systems worldwide follow the protection standards as stated in U.S. National Electric Code (NEC) or International Electro-Technical Commission (IEC) to use Over-Current Protection Device (OCPD) and Ground Fault Protection Device (GFPD) for detection and clearing of short-circuit faults like LL and LG faults respectively. But due to the operation of Maximum Power Point Tracking (MPPT), blocking diodes in the PV system and environmental conditions, conventional OCPD and GFPD often fail to detect LL fault in particular for most of the cases. Hence, the researchers have discussed various protection challenges in solar PV systems and also developed a fault detection method for LL faults only as in [5–7]. Further Outlier detection rules as mentioned in [8, 9] are developed based on measurement of instantaneous string current to identify the faults in PV system. The fault detection methods also developed based on the digital twin approach [10], and based on the magnitudes and changing pattern of first and last module voltages in each string [11]. Further, A. F. Murtaza et al. [12] used the measured incoming and outgoing current data from each string to identify the PV faults. However, all these methods require more number of sensors, controllers and additional hardware setups. Hence, the overall cost and complexity of the system increased.

The fault identification method given in [13] uses machine learning techniques like graph-based semi-

***Corresponding author: Senthil Kumar Subramaniam**, Department of Electrical and Electronics Engineering, National Institute Technology, Tiruchirappalli, Tamilnadu, India, E-mail: skumar@nitt.edu
Namani Rakesh, Sanchari Banerjee and Natarajan Babu: Department of Electrical and Electronics Engineering, National Institute Technology, Tiruchirappalli, Tamilnadu, India,
E-mail: namanirakesh@rgukt.ac.in (N. Rakesh),
sanchari.banerjee.95@gmail.com (S. Banerjee), dlc@nitt.edu (N. Babu)

supervised learning to classify the faulty operating conditions. Akram, M. N., and Lotfifard, S. [14] developed a Probabilistic Neural Network (PNN) method to detect the faults in PV system. The PNN method uses manufacturer's datasheet values to build a correlation among the ideality factor and series resistance with temperature respectively which helped in the identification of faults. The detection methods in [8, 13] require voluminous data of the PV array, and the specific design of PV plant installation, which are quite non-feasible, and have limited applications in case of large PV systems. Further the authors have proposed a method using comparison between the values of measured and AC output power through model prediction in order to identify the faults in PV system [15, 16]. Hu, Y. et al. [17] proposed a method to optimize the placement of voltage sensor to identify faults. It was found that integrating sensors with the available power converters in the PV market were a very tough task. Hariharan, R. et al. [18] proposed a method using two variables such as array losses and gamma, which calculate the difference in power losses of the PV array and instantaneous ratios of power by irradiation in order to detect LL faults and also for PSC (partial shaded condition). For the calculations of the aforementioned variables, the PV system was observed for the values of current, voltage and insolations. Further the authors used a change in MPP values and dissimilarity in voltage and power ratios respectively to detect faults [19, 20]. Yi, Z. and Etemadi, A. H. [21] employed a technique called Multi-resolution Signal Decomposition (MSD) and fuzzy inference system to detect whether a fault has happened or not in the PV system. Chen, L. et al. [22] employed an Auto Regressive (AR) model to measure time correlation in the output signals of PV system to describe the faulty signal. Kumar, B. P. et al. [23] proposed a method to identify faults based on the observed current and voltage data points of PV array using Wavelet Packet Transforms (WPTs) technique. The WPT technique requires expensive software/hardware platforms and also it is difficult to integrate with the existing systems.

Roy, S. [24] developed a new technique like Spread Spectrum Time Domain Reflectory (SSTDR) based on variation in impedance during faults to detect LG faults. It has a problem like the assessment of results had done on a baseline which depends on the number of strings present in the PV system and also the location of fault from the device. Pillai, D. S. et al. [25] developed a method to detect the faults using the existing P&O MPPT tracking operation. This method does not require any sensors during the detection process. The developed method considers the effects of varying temperatures and irradiances. However it excludes the effects of blocking diodes used in PV system during the faults. The comparative assessment of various existing fault detection approaches in PV systems is given in [26]. The fault detection methods existing so far developed using various parameters and techniques are able to detect mainly LL fault and PSC only. After a detailed literature survey, the authors have identified the following one or more problems in fault detection algorithms: (i) Problem in segregating the faults and partial shading conditions, (ii) Lack of compatibility with the existing MPPT methods, (iii) Necessity of added hardware and/or sensors, (iv) Ample data requirement, (v) Energy loss due to the fault detection with insufficient data about number of faulty modules and strings.

Hence, to address the above mentioned problems, the proposed method has developed with the following contributions: (i) PV array fault detection for dynamic change in irradiation, (ii) Identifying and segregating the faults between the LL and partial shading conditions, (iii) Status of PV array with type of fault such as LL or PSC, (iv) Number of mismatch modules (or Short circuited bypass diodes), (v) Number of mismatch strings (or Open circuited blocking diodes), (vi) Avoided additional requirement of sensors and hardware requirement, (vii) Compatible with existing MPPT methods.

This paper presents a new detection method which works in two phases. In the first phase, it detects the type of fault using three variables, namely gamma (γ) for LL fault detection and relative change in irradiation (G_r) and array losses (Lar) for PSC. In the second phase, it finds the number of mismatch modules and mismatch strings after L-L fault is detected in the PV system.

The organization of the paper as follows: Section 3 discusses the analysis of faults with and without blocking diodes in grid-connected PV system. Section 4 elaborates the analysis of the proposed method with methodology to find the faults and partial shade conditions and also with the methodology to find the number of mismatch modules and strings. Section 5 illustrates the algorithm and flowchart of the proposed method. Section 6 depicts the discussion about the experimental and simulations results with comparative assessment. Finally, the briefings of the investigations are given in Section 7.

2 Mathematical modeling of PV cell

The mathematical model used for a PV cell design in MATLAB/simulink is developed using equations as given in [27]. The specifications of the PV module used in MATLAB/simulink are given in Table 1.

Table 1: Specifications of the PV Module and 3 × 2 PV array.

Parameters	Symbol	PV module rating 3 × 2 PV array rating
Maximum power	P_m	51 W 306 W
Maximum power current	I_{mp}	2.88 A 5.76 A
Maximum power voltage	V_{mp}	17.7 V 53.1 V
Open-circuit voltage	Voc_{SYS}	21.4 V 64.2 V
Short-circuit current	Isc_{SYS}	3.24 A 6.48 A
Series resistance	R_s	0.075 Ω
Shunt resistance	R_{sh}	100 Ω

3 Fault analysis in grid connected PV system

3.1 Analysis of faults with and without blocking diodes

The faults in PV system occur at various locations such as PV array, power converter and utility grid. The PV array faults such as LL faults occur between string one and string two of the PV system as shown in Figure 1(a).

Figure 1(b) shows the Current versus Voltage (I-V) characteristic curve of the PV system without blocking diodes and its string current at prefault and postfault conditions along with the fault current (I_F). It is observed from Figure 1(a) and Figure 1(b) that a L-L fault reverses the flow of current through the faulty string. The faulty string generates a I_F between the points F_1 and F_2, while the other healthy string generates a back or reverse current (I_{REV}) that flows into the faulty string.

From Figure 1(b), it is observed that the I_F at the instant of fault is almost twice the short-circuit current of the string at prefault condition and hence it can be easily detected by the OCPDs used in the PV system. The grid-connected PV system with blocking diodes under fault condition is shown in Figure 2(a). The I-V characteristic curve of the PV system with blocking diodes and string current at prefault and postfault conditions along with the I_F is as shown in Figure 2(b). The faulty string generates a I_F between the points F_1 and F_2, while the back or I_{REV} generated by the other healthy string is blocked by the blocking diode from flowing into the faulty string.

The instant I_F is almost equal to the short-circuit current of the string at prefault state as shown in Figure 2(b), because the I_{REV} is blocked with the blocking diodes. Hence, the I_F does not meet the threshold current of OCPDs and thus the fault remains undetected in the PV system. Moreover, the MPPT operation of the power converter often changes the operating point to a new position on the I-V characteristic curve such that the I_F magnitude decreases over the time. If the L-L fault occurs under low irradiation conditions such as during sunrise or sunset, the I_F through the affected strings is found to be not large enough to meet the threshold limit of the OCPDs, and thus the fault remains undetected.

4 Analysis of the proposed method

4.1 Methodology to find LL fault and partial shade conditions

The Grid-connected PV system with various types of faults is as shown in Figure 3. To understand the effects of L-L faults and PSC in a Grid-connected PV system, it is designed with the specifications of the individual PV module as given in Table 1 and simulated in MATLAB/simulink.

The Power versus Voltage (P-V) and I-V characteristic curves at prefault and postfault conditions at Standard Testing Conditions (STC) as Temperature (T) of 25 °C and irradiance (G_O) of 1000 W/m^2 are shown in Figure 4. It is observed that the postfault power of the PV system at the Maximum Power Point (MPP) is less than that of the prefault power which is found to be equal to 91.6 W. To measure the instantaneous change in the power due to fault, a variable Gamma (γ) is used which is defined as ratio of the instantaneous power of the PV system to the instantaneous irradiation falling on the PV system with a unit of m^2.

$$\text{Gamma}\,(\gamma) = \frac{P_{PV}}{G} = \frac{V_{PV} \times I_{PV}}{G} \tag{1}$$

Based on the P-V characteristic curve in Figure 4 and using Equation (1), the threshold value for the change in gamma (γ) is taken as 0.09 m^2. The least power loss occurs from a PV system when atleast one of the modules in PV system is partially shaded. Therefore to understand the effects of partial shading, only one module of the designed Grid-connected PV system has been shaded as shown in Figure 3. The corresponding P-V and I-V simulation characteristic curves of the PV system with one module partial shade condition with three different irradiations are as shown in Figure 5.

The least power drop in a PV system caused during LL fault with one module mismatch has been excluded the effect of PSC. Based on the P-V and I-V curves of the PV system as shown Figure 5, the value of gamma and the change in value of gamma is calculated for each PSC from the prefault to postfault condition as given in Table 2.

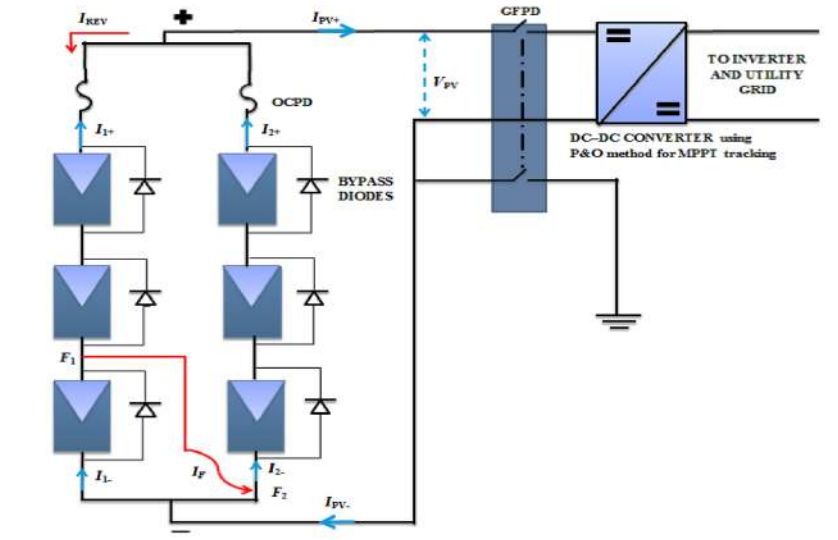

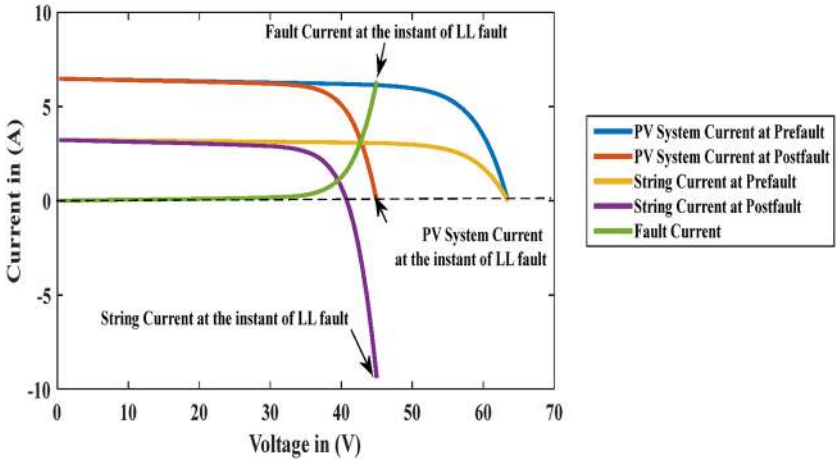

Figure 1: (a). Grid-connected PV System without blocking diodes under fault. (b). I-V Characteristic curve without blocking diodes under fault.

$$\text{Change in Gamma } (\Delta y) = \text{Prefault value of gamma} - \text{Postfault value of gamma} \quad (2)$$

For low irradiation condition of below 400 W/m^2 as given Table 2, the PV system power loss is almost same as that of one module-mismatch.

Therefore, it is important to find a way to detect whether the power loss is due to PSC or LL fault. To detect the partial shading condition, two variables are used namely, approximate array losses (Lar) and G_r.

Approximate array loss (Lar) is derived as the difference between the estimated power and actual power of the PV array and it has a unit of Watt.

$$\text{Estimated Power } (P_{\text{estimated}}) = \text{Maximum Power} \times \frac{\text{Instantane ous Irradiation}}{\text{Irradiation at STC}} = P_m \times \frac{G}{G_O} \quad (3)$$

$$\text{Actual Power } (P_{\text{actual}}) = P_{\text{PV}} = V_{\text{PV}} \times I_{\text{PV}} \quad (4)$$

$$\text{Approximate array losses (Lar)} = P_{\text{estimated}} - P_{\text{actual}} = P_m \times \frac{G}{G_O} - (V_{\text{PV}} \times I_{\text{PV}}) \quad (5)$$

G_r is derived as the ratio of the difference in irradiation at STC and instantaneous irradiation to the irradiation at STC and it is unit less, which is expressed as:

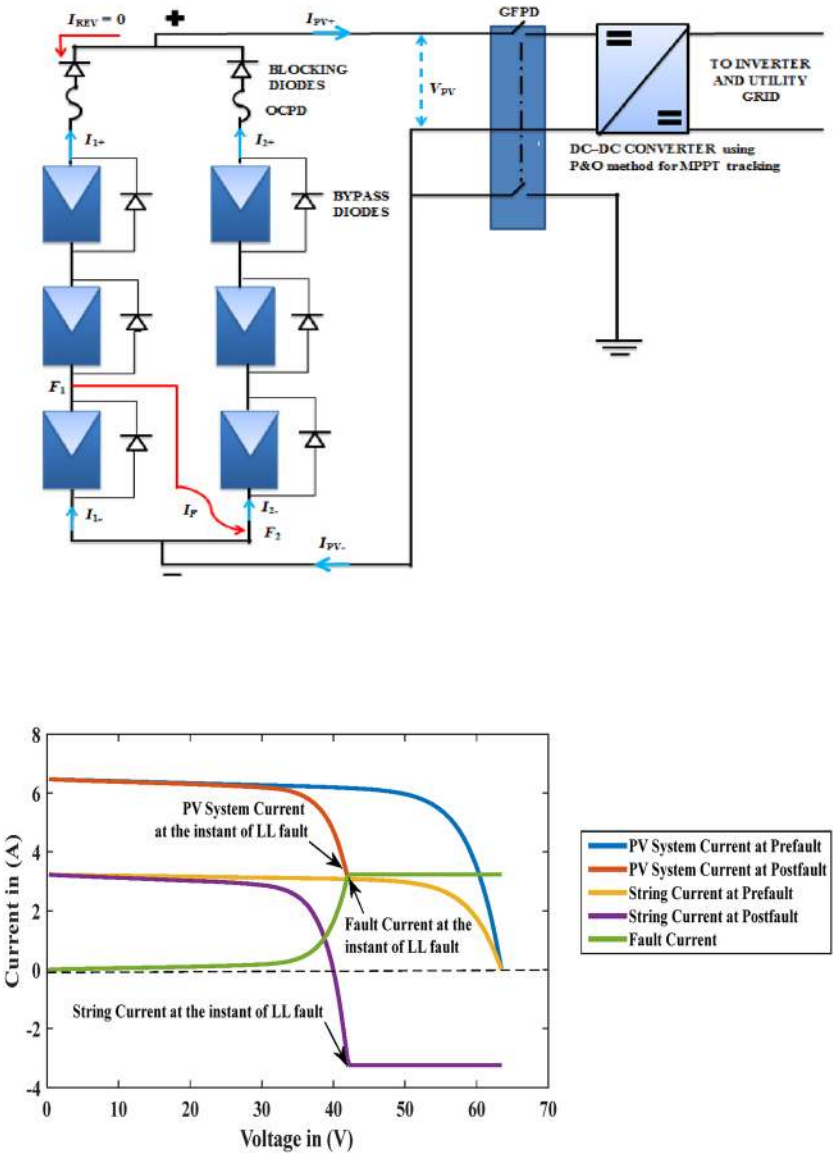

Figure 2: (a). Grid-connected PV System with blocking diodes under fault. (b). I-V Characteristic curve with blocking diodes under fault.

$$\text{Relative change in irradiation}\,(G_r) = \frac{\text{Irradiation at STC} - \text{Instantaneous Irradiation}}{\text{Irradiation at STC}} = \frac{G_O - G}{G_O} \quad (6)$$

Based on the P-V and I-V characteristic of the PV system from Figure 5, the value of approximate array loss (Lar) and G_r are calculated for different cases as given in Table 3. In each case, the maximum power from the P-V curve is taken as actual power of the PV system.

From Table 3, it is observed that the approximate array loss (Lar) in PSC II is almost same as that of LL fault with one module mismatch but the G_r is found to be almost zero. Thus, the two variables together are used to identify whether the power loss in a PV system is due to the partial shading or not. The constant parameters used to find LL fault and partial shade conditions are derived from the above equations as given in Table 4. Based on the PV system condition and type of faults, the statuses of the faults are denoted as mentioned in Table 5.

4.2 Methodology to find the number of mismatch modules and strings in PV system

The variables like Number of mismatch modules (n), Voltage drop (V_k), Number of mismatch strings (m), Current drop (I_k) and the corresponding error constants are

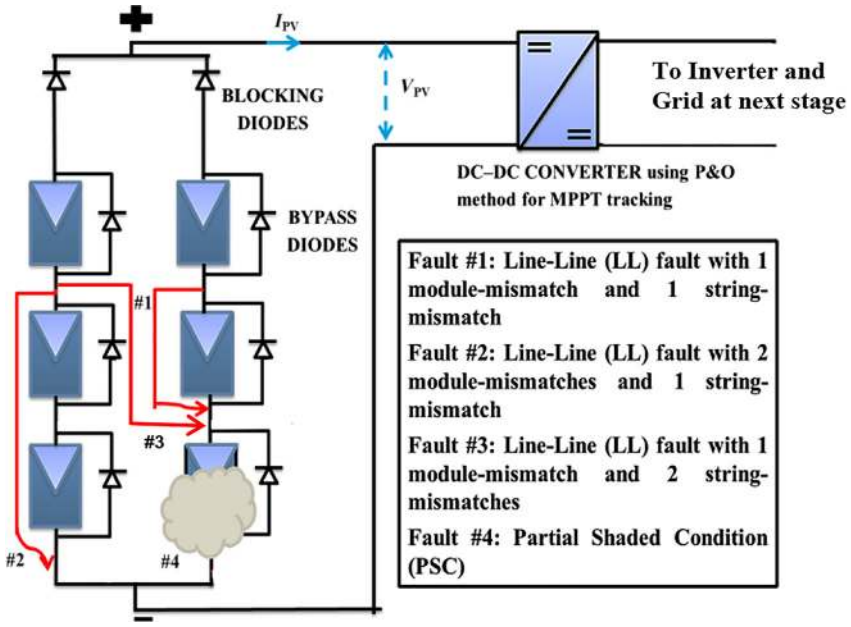

Figure 3: Grid-connected PV System with various types of faults.

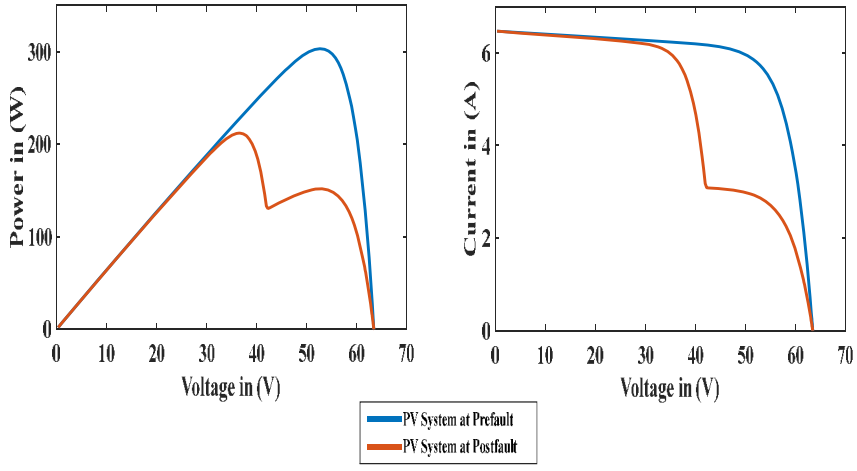

Figure 4: P-V and I-V characteristic curves at prefault and postfault conditions.

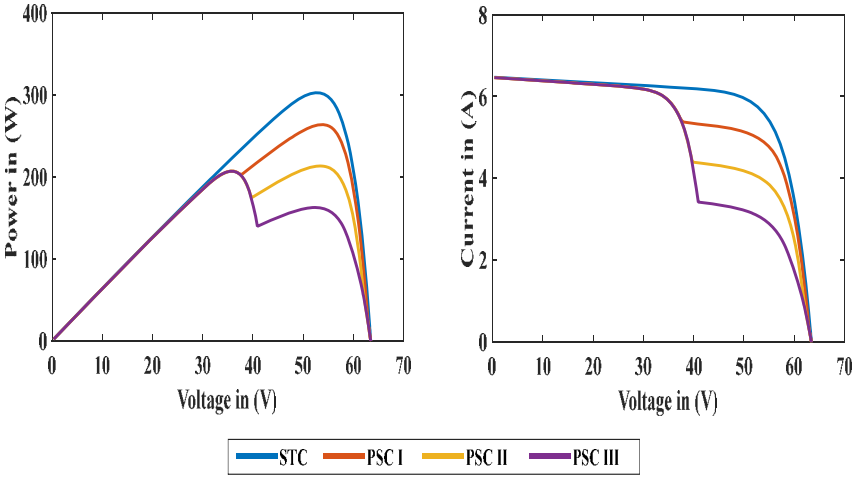

Figure 5: P-V and I-V curves of the PV system under various partial shaded conditions (PSC).

Table 2: Gamma and change in gamma for various PSCs.

PSC	Gamma (γ)	Change in gamma
I	0.249 m^2	0.054 m^2
II	0.183 m^2	0.12 m^2
III	0.207 m^2	0.096 m^2

Table 3: Lar and G_r for various PSCs.

PSC	Approximate array loss (Lar)	Relative change in irradiation (G_r)
I	38.69 W	0.05
II	89.55 W	0.1
III	50.46 W	0.15

G_r, Relative change in irradiation; Lar, Approximate array loss; PSCs, partial shaded conditions

Table 4: Constant parameters used to find LL fault and partial shade conditions.

Parameters	Formula used	Value
ε_1	Least value of G_r	0.05
ε_2	80% of least value of Lar	30.95 W
ε_3	−(Threshold value for the change in gamma (γ) in one module mismatch under LL fault)	−0.09 m^2

Table 5: Status of PV System fault.

PV system condition	Status of PV system fault
Normal operating condition (STC)	0
Line-line fault	1
Partial shaded condition (PSC)	2

developed very clearly with strong mathematical derivations and observations from I-V characteristics of PV array.

4.3 Effect of mismatched modules and strings in PV Array under LL fault

It is observed that the drop in the value of voltage during LL fault is almost equal to the product of the number of mismatched modules and the open-circuit voltage of one PV module. Similarly the drop in current on the onset of fault is found to be equal to the product of the number of mismatched strings and the short-circuit current of one PV module. To analyse the above mentioned condition, a PV array of 5×4 is designed using the specification of PV module mentioned in Table 1 and simulated for different cases of mismatched modules and strings in the following two ways.

i. String-mismatch is kept constant while varying modules mismatches and the I-V Characteristic curves obtained for each case as depicted in Figure 6.
ii. Module-mismatch is kept constant while varying strings mismatches and the I-V Characteristic curves obtained for each case as depicted in Figure 7.

Based on the obtained I-V characteristic curves for all cases, the drops in voltage and current are calculated in order to find the number of mismatch modules and number of mismatch strings using the following formulae.

$$\begin{aligned}\text{Voltage drop}\,(V_k) = {} & \text{Open} \\ & - \text{circuit voltage of the PV system}\,(\text{Voc}_{\text{SYS}}) \\ & - \text{Instantaneous PV system voltage}\,(V_{\text{PV}})\end{aligned} \tag{7}$$

$$\text{Number of mismatch modules}\,(n) = \frac{\text{Voltage Drop}\,(V_k)}{\text{Open} - \text{circuit voltage of one module}\,(\text{Voc}_m)} \tag{8}$$

$$\text{Error in the value of number of mismatch modules}\,(e_1) = n - \text{round of } n \tag{9}$$

$$\begin{aligned}\text{Current drop}\,(I_k) = {} & \text{Short} \\ & - \text{circuit current of the PV system}\,(\text{Isc}_{\text{SYS}}) \\ & - \text{Instantaneous PV system current}\,(I_{\text{PV}})\end{aligned} \tag{10}$$

$$\text{Number of mismatch strings}\,(m) = \frac{\text{Current Drop}\,(I_k)}{\text{Short} - \text{circuit current of one module}\,(I_{\text{SCm}})} \tag{11}$$

$$\text{Error in the value of number of mismatch strings}\,(e_2) = m - \text{round of } m \tag{12}$$

The obtained results from the calculations given in Table 6 help in deriving the range of approximate error values of e_1 and e_2 for finding the number of mismatch modules and number of mismatch strings in the grid-connected PV system. The calculated errors e_1 and e_2 have not considered the effect of MPPT tracker operation in its calculations. Thus, the designed PV system is simulated with MPPT tracker using P&O method in MATLAB/Simulink. It is observed that the effect of MPPT operation, changes the error e_1 to $\pm$ 0.5 while the error e_2 remains almost same as given in Table 4. Based on the

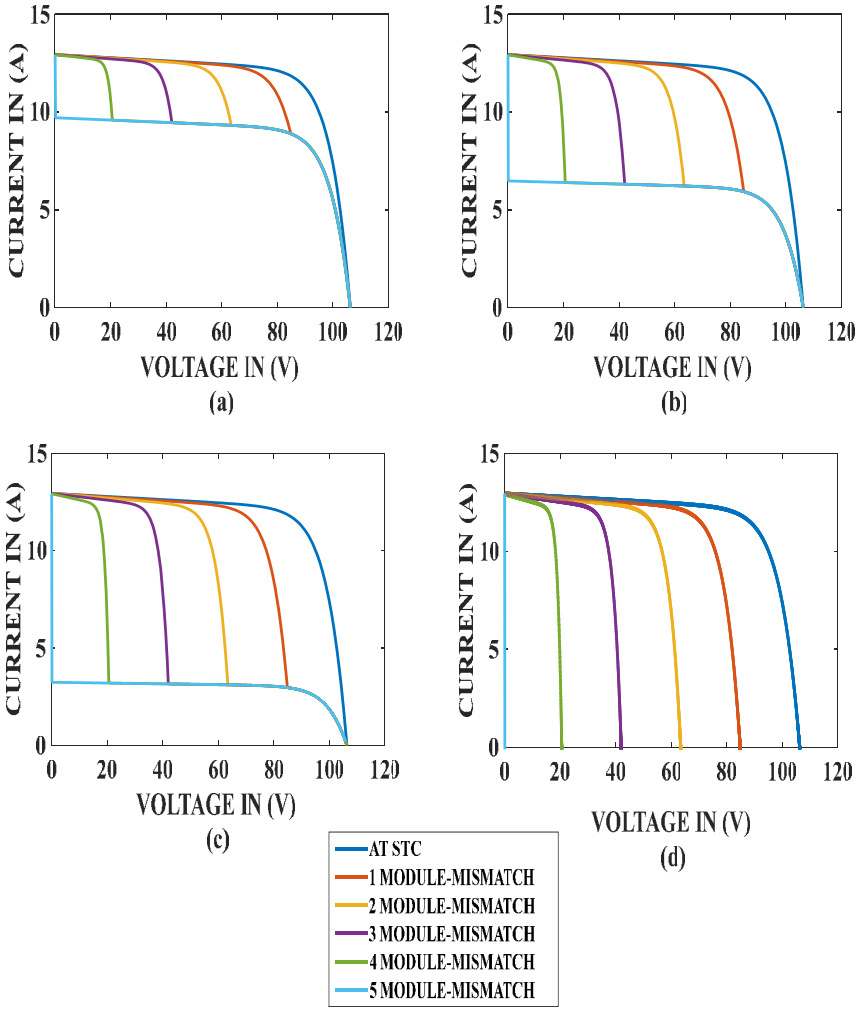

Figure 6: I-V Characteristic curves of the PV System with varying module-mismatches while keeping string-mismatch constant at (a) One string-mismatch, (b) Two string-mismatches, (c) Three string-mismatches and (d) Four string-mismatches.

calculations as given in Table 6 and simulations results as given Figure 6 and Figure 7, the corrected range of error values εr_1 and εr_2 are derived for finding the number of mismatch modules and strings in the grid-connected PV system as given in Table 7.

5 Proposed fault detection method for grid connected PV system

Based on the analysis given in Section 4, a new fault detection method is developed to know the number of mismatch modules (or short-circuited bypass diodes) and mismatch strings (or open-circuited blocking diodes) along with the status of L-L fault and PSC. Hence, it can differentiate whether the power drop in PV system is due to PSC or LL fault. Further, the power loss can be estimated by knowing the number of mismatch modules and strings in PV system. The detailed step by step approach of the proposed fault detection method is given with an algorithm in Section 5.1 and it is illustrated with flow chart as given in Figure 8. The derived error values from the calculations as given in Table 4 and Table 5 are used in the proposed detection method. Further the fault status representation using the proposed detection method is given in Table 6.

5.1 Algorithm for proposed fault detection method

The flowchart of the proposed method to detect faults in PV system as shown in Figure 8 is explained with an algorithm as follows:

Step 1: The instantaneous value of voltage, current and irradiation falling on the PV system are measured and stored.

Step 2: The values of y, Lar and G_r are calculated using Equations (1), (5) and (6) respectively from the stored values in Step 1.

Table 6: Calculated values obtained from the I-V characteristics of Figure 6 and Figure 7.

Strings mismatch	Modules mismatch	V_k (V)	N	e_1	I_k (A)	m	e_2
1	1	21.509	1.005	0.005	4.050	1.250	0.250
	2	42.960	2.007	0.007	3.601	1.111	0.111
	3	64.358	3.007	0.007	3.474	1.072	0.072
	4	85.847	4.012	0.012	3.193	0.985	−0.015
	5	106.224	4.964	−0.036	3.236	0.999	−0.001
2	1	21.520	1.006	0.006	6.966	2.150	0.150
	2	42.901	2.005	0.005	6.722	2.075	0.075
	3	64.341	3.007	0.007	6.583	2.032	0.032
	4	85.747	4.007	0.007	6.500	2.006	0.006
	5	106.224	4.964	−0.036	6.472	1.998	−0.002
3	1	21.463	1.003	0.003	9.950	3.071	0.071
	2	42.888	2.004	0.004	9.787	3.021	0.021
	3	64.294	3.004	0.004	9.755	3.011	0.011
	4	85.733	4.006	0.006	9.558	2.950	−0.050
	5	106.224	4.964	−0.036	9.708	2.996	−0.004
4	1	21.418	1.001	0.001	12.936	3.993	−0.007
	2	42.833	2.002	0.002	12.942	3.995	−0.005
	3	64.250	3.002	0.002	12.943	3.995	−0.005
	4	85.668	4.003	0.003	12.943	3.995	−0.005
	5	106.224	4.964	−0.036	12.943	3.995	−0.005
1	1	21.509	1.005	0.005	4.050	1.250	0.250
2		21.520	1.006	0.006	6.966	2.150	0.150
3		21.463	1.003	0.003	9.950	3.071	0.071
4		21.415	1.001	0.001	12.941	3.994	−0.006
1	2	42.960	2.007	0.007	3.601	1.111	0.111
2		42.901	2.005	0.005	6.722	2.075	0.075
3		42.888	2.004	0.004	9.787	3.021	0.021
4		42.833	2.002	0.002	12.943	3.995	−0.005
1	3	64.358	3.007	0.007	3.474	1.072	0.072
2		64.341	3.007	0.007	6.583	2.032	0.032
3		64.294	3.004	0.004	9.755	3.011	0.011
4		64.252	3.002	0.002	12.937	3.993	−0.007
1	4	85.847	4.012	0.012	3.193	0.985	−0.015
2		85.747	4.007	0.007	6.500	2.006	0.006
3		85.733	4.006	0.006	9.558	2.950	−0.050
4		85.668	4.003	0.003	12.942	3.995	−0.005
1	5	106.224	4.964	−0.036	3.236	0.999	−0.001
2		106.224	4.964	−0.036	6.472	1.998	−0.002
3		106.224	4.964	−0.036	9.708	2.996	−0.004
4		106.224	4.964	−0.036	12.943	3.995	−0.005

Step 3: The variable y_m is used to detect the duration of fault in the PV system after the onset of LL fault. Initially it is set to zero. Also a variable "Chk" is used to flow the control of the algorithm to step 8 in order to detect the number of mismatch modules and strings in the faulty PV system. Initially it is set to zero.

Step 4: The variables Δy_1 and Δy_2 are computed using the expression for Δy_1, which is the difference between the value of gamma for ith and $(i-1)^{th}$ samples and Δy_2 is the difference between the value of gamma for ith sample and y_m.

Step 5: If the G_T and array losses (Lar) are more than or equal to ε_1 and ε_2 respectively, then it is a PSC else jump to Step 6.

Step 6: If the value of Δy_1 is lesser than or equal to ε_3, then it is under LL fault condition and set $y_m = y_{i-1}$ and Chk = 1. In order to check whether the change in the value of y is due to fault or not, the control jumps to Step 7 in the next cycle.

Step 7: If the value of Δy_2 is lesser than or equal to ε_3, then it is under LL fault condition and set Chk = 1. If not, then the system is under normal operating condition. After this, the control goes back to Step 1.

Step 8: If the PV system is detected to be under LL fault in Step 6 and 7, the control jumps to Step 8. In this step, the

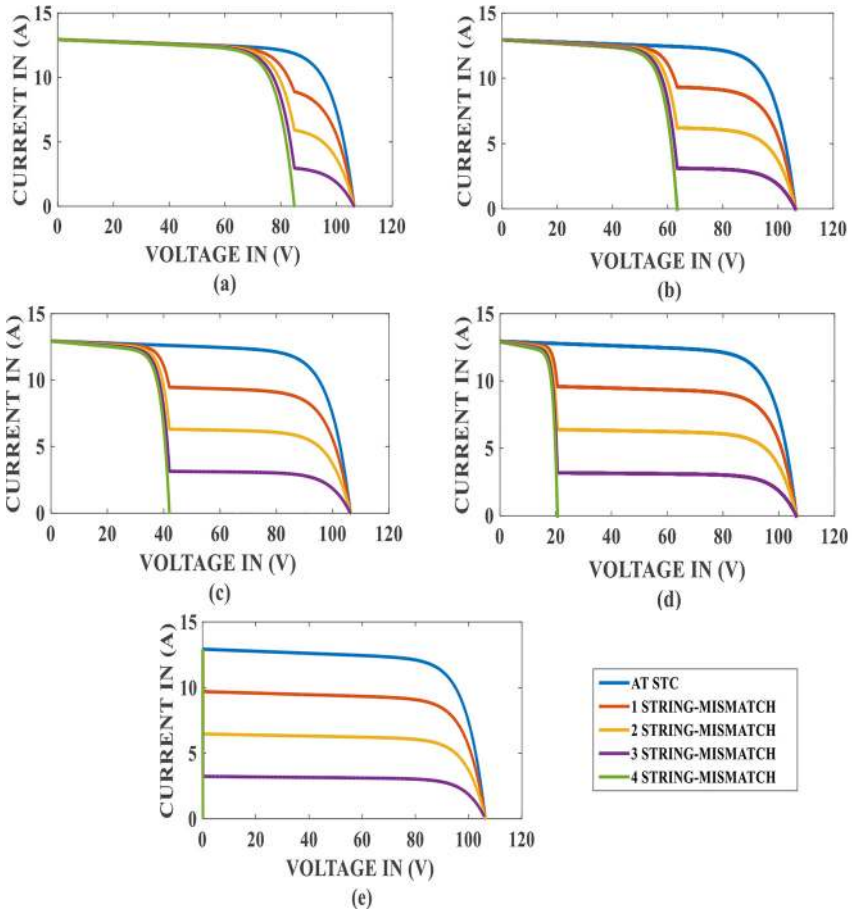

Figure 7: I-V Characteristic curves of the PV System with varying string-mismatches while keeping module-mismatch constant at (a) One module-mismatch, (b) Two module-mismatches, (c) Three module-mismatches, (d) Four module-mismatches and (e) Five module-mismatches.

Table 7: Constant parameters used to find the number of mismatch modules and strings.

Parameters	Minimum value	Maximum value
εr_1	−0.5	0.5
εr_2	−0.05	0.25

instantaneous value of system voltage, system current and the variable Chk are measured and stored.

Step 9: Initialization of variable as per PV system as Voc, Isc, Vp, Ip and n_2=n=m_2=m=0. Here the variables Voc and Isc store the open-circuit voltage and short-circuit current of the PV system. While the variables Vp and Ip store the open-circuit voltage and short-circuit current of one module of the PV system. The variables n_2 and n are used to store the number of mismatch modules whereas the variables m_2 and m store the number of mismatch strings.

Step 10: The variables V_k, n_1, e_1, I_k, m_1 and e_2 are computed by equations (7)–(12) using the stored values of system voltage and system current in step 8 and set variables in Step 9.

Step 11: If Chk is equal to one, then the control jumps to Step 12. If not, then set the variables "n" and "m" equal to zero and the control jumps to Step 8 and the fault detection algorithm goes to Step 1.

Step 12: If the condition in Step 11 is satisfied, the error parameters e_1 and e_2 calculated in Step 10 are check. If the error parameters e_1 and e_2 lie in the range of ($\varepsilon r_{1min} \leq e_1 \leq \varepsilon r_{1max}$) and ($\varepsilon r_{2min} \leq e_2 \leq \varepsilon r_{2max}$) respectively, then jump to Step 13. If not, then set the variables "n" and "m" equal to zero and the control jumps to Step 8.

Step 13: The variables n_1 and m_1 are set as (n_1–e_1) and (m_1–e_2) respectively and the control goto to Step 14.

Step 14: The variables n_2 and m_2 are used to store the number of mismatch modules and strings of the PV system at the onset of fault. Because of MPPT tracking, the value of n_1 and m_1 varies. It is seen that only at the onset of fault, the maximum drop in voltage and current in the PV system are reached. Therefore to get the correct value, it is checked that whether n_2 is less than n_1 as well as m_2 is less than m_1 or not. If the condition is satisfied, then set $n_2 = n_1$and $m_2 = m_1$;

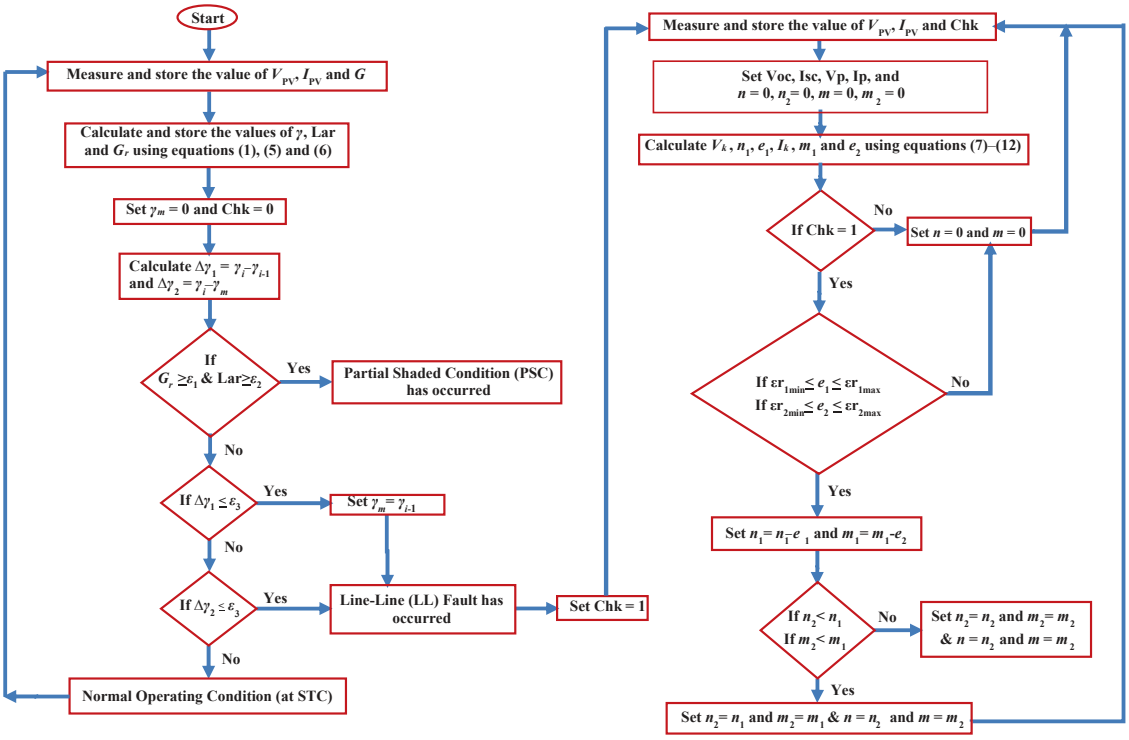

Figure 8: Flowchart for the proposed method to detect faults in PV system.

else the variables n_2 and m_2 remain unchanged. Hence the variables n_2 and m_2 will give the correct number of mismatch modules and strings of the PV system when L-L fault occurs. The values obtained in n_2 and m_2 are stored in "n" and "m" respectively and the control then jumps to Step 8.

6 Results and discussions

The small scale PV grid connected experimental set-up as shown in Figure 9 is used to validate the MATLAB/Simulink simulation results. For better validation of the proposed method, the PV modules with the specifications as given in Table 8 are used in the experimentation, which are close to the PV modules with the specifications as given in Table 1 used in MATLAB/Simulink simulations. The grid-tied inverter incorporates the Perturb & Observe (P&O) MPPT algorithm. The specifications of grid-tied inverter are given in Table 9. The PV array by 3×2 modules in series-parallel connections is used for experimentation and also for MATLAB/Simulink simulation. The specifications of each PV module and its corresponding accessories are shown in Table 8. The halogen lamps are used to create the artificial light source on PV modules. The light intensity on PV modules is controlled from 976.13 to 626.23 W/m^2 using the halogen regulator to create the partial shade conditions. The toggle switches are used to create the required faults by connecting lines between the strings and modules as performed in MATLAB/Simulink simulations. The faults are created at 12 h 04 min in experimentation by turn ON/OFF switches for all type faults considered in this work. The Data Acquisition Unit is used to record the necessary data from PV array.

The proposed method to know the number of mismatch modules (or short-circuited bypass diodes) and mismatch strings (or open-circuited blocking diodes) along with the status of L-L fault and PSC are tested with MATLAB/Simulink simulations and also on small scale laboratory developed grid connected PV system for four different fault conditions in grid-connected PV system as given in Figure 3. Further, the discussions on corresponding simulation and experimental results have been discussed in Case 1 to Case 4. The comparative assessment of the proposed method is given in Table 10 to shows the advantages over the existing methods by finding the number of mismatch modules and mismatch strings in grid-connected PV system.

Case 1: L-L fault with one module-mismatch and one string-mismatch

The effect of one module-mismatch and one string-mismatch is tested on a grid-connected 3×2 PV system both on MATLAB/Simulink simulation and experimentation with the connections as shown in Figure 3. The simulation and experimental results are as shown in Figure 10. It is observed that at 0.2 s in simulation and at 12 h 04 min in experimentation, there is a sudden drop in y which is less than the threshold value of "ε_3". Hence, the status of the PV system has been observed with "1" in Figure 10. This indicates that LL fault has occurred in PV system. Further, it gives the information about the number of module-mismatches and string-mismatches equals to "1" as shown in Figure 10.

- The value of y keeps on changing gradually till it settles to a value at the prefault state. However, when fault occurs in the PV system, y drops sharply from 0.303 to 0.151 m^2 in simulation and 0.220–0.08 m^2 in experimentation. Thus, the change in y occurrence in simulation and experimentation at the moment of fault is found to be 0.152–0.14 m^2 respectively. This is more than the prescribed threshold value of 0.09 m^2. Then the change in y after the instant of fault reduces to a value of 0.0918 m^2 with respect to the prefault value of 0.303 m^2 which is also greater than 0.09 m^2.
- There is a sudden drop in the PV system current and then it gradually restores to its previous value.
- There is a sudden drop in PV power at the instant of fault, then it gradually restores to a low power value of 211.5–172 W both in simulation and experimentation respectively.

Table 8: PV module and its corresponding accessories specifications.

Parameters	Specification
Maximum power	43.84 W
Maximum power current	2.39 A
Maximum power voltage	18.33 V
Open-circuit voltage	22.25 V
Short-circuit current	2.53 A
Type	Poly-crystalline
Fill factor	0.78
Efficiency of module	14.19%
Efficiency of cell	17.95%
Halogen lamps	six per each module
Power rating each	150 W
Halogen regulator power rating	4500 W
Radiation metre range	0 to 1999 W/m^2

Table 9: Grid tied inverter specifications.

Parameters	Specification
Maximum power point voltage range	45–100 V
Rated grid voltage	230 V
Maximum output current	2.5 A
Rated power	500 W
Feeding phases	Single phase

Case 2: L-L fault with two module-mismatches and one string-mismatch

The designed grid-connected PV System is simulated in MATLAB/simulink along with experimentation for

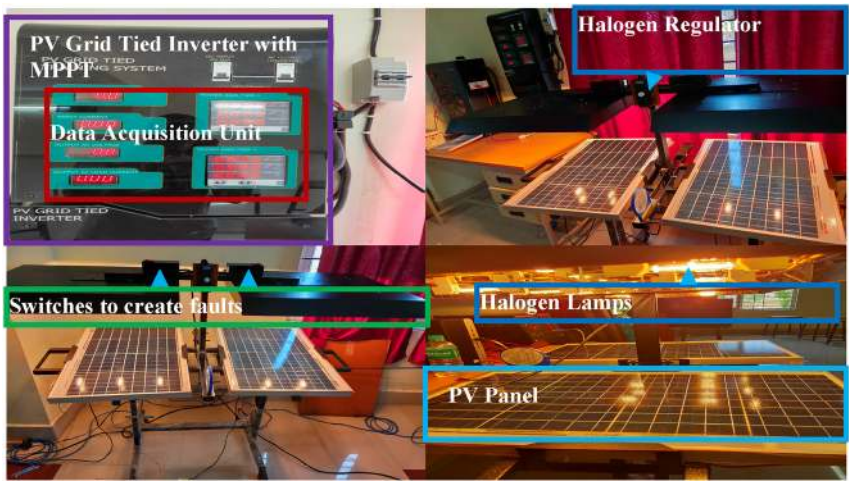

Figure 9: Experimental set-up of the PV system.

Table 10: Comparative assessment of the proposed method.

Performance parameters	Fault detection methods		
	[10]	[18]	Proposed method
Permanent fault detection (L-L and L-G)	Yes	Yes	Yes
Temporary fault detection (partial shading)	No	Yes	Yes
Status of the fault	No	Yes	Yes
Finding the number of short-circuited or mismatch modules	No	No	Yes
Finding the number of short-circuited or mismatch strings	No	No	Yes

analysing the effects of LL fault with two module mismatches. The results of both simulation and experimentation are as shown in Figure 11. It is observed that at the instant of fault, there is a sudden drop in γ which is less than the threshold value of "ε_3". Hence, the status of the PV system has been observed with "1" in Figure 11. This indicates that LL fault has occurred in PV system. Then the proposed method to detect faults in PV system gives the number of module-mismatches equals to "2" and the number of string-mismatches equals to "1" as shown in Figure 11.

- The value of γ initially keeps on changing gradually till it settles to a value before the occurrence of fault. At the moment of fault, γ drops suddenly from 0.303 to 0.1 m^2 and 0.235–0.1 m^2 in both simulation and experimentation respectively. Therefore the net drop in gamma is 0.203–0.135 m^2 respectively which is much greater than 0.09 m^2. It is observed that the change in the value of γ is settle at a value which is also found to be greater than the threshold value for the change in γ i.e., 0.09 m^2.
- After the occurrence of fault, the PV system current shows a sudden drop at the instant of fault and afterwards it follows a low value of current around 3.3 and 3.2 A both in simulation and experimentation respectively.

Case 3: L-L fault with one module-mismatch and two string-mismatches

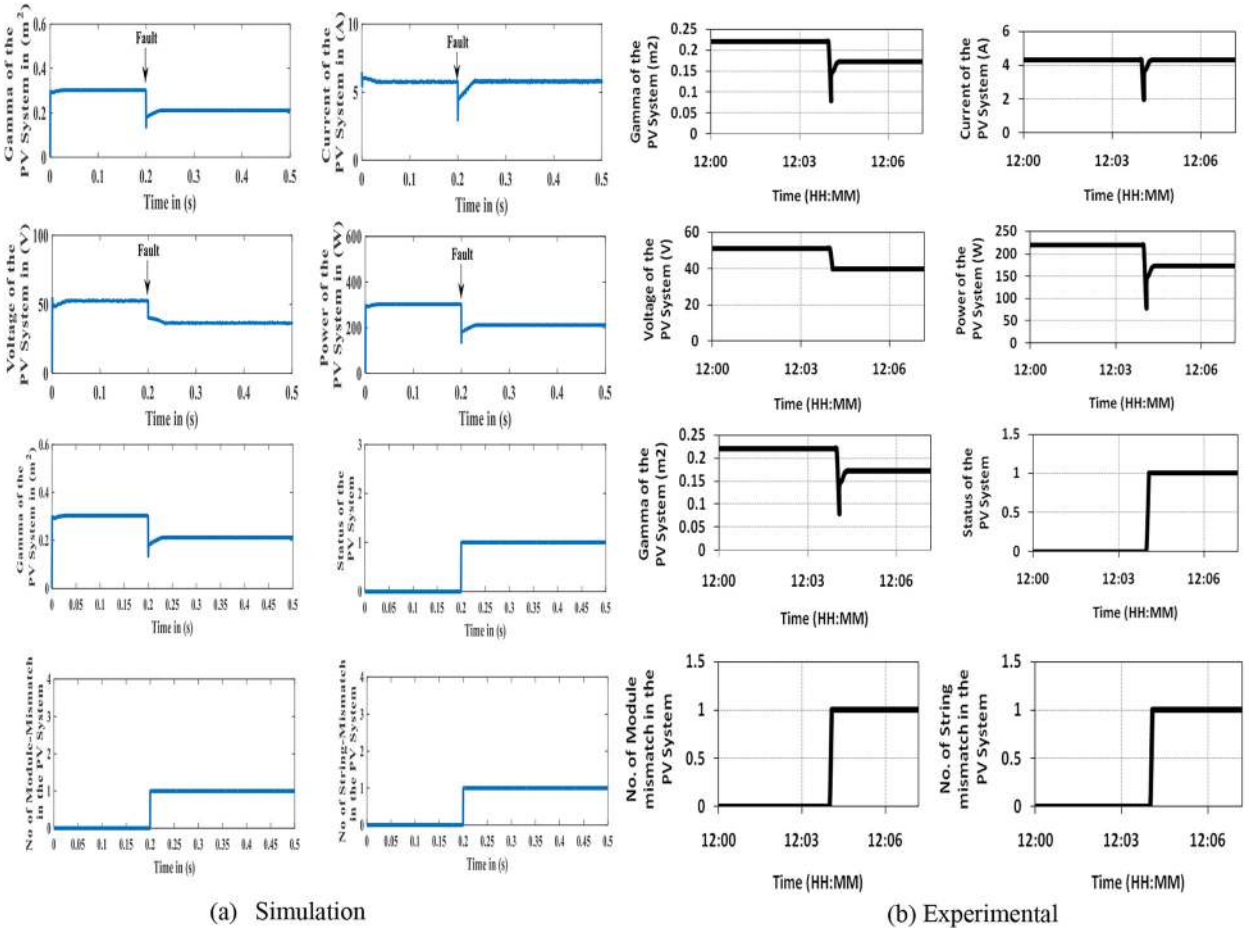

Figure 10: LL fault with one module-mismatches and one string-mismatch.

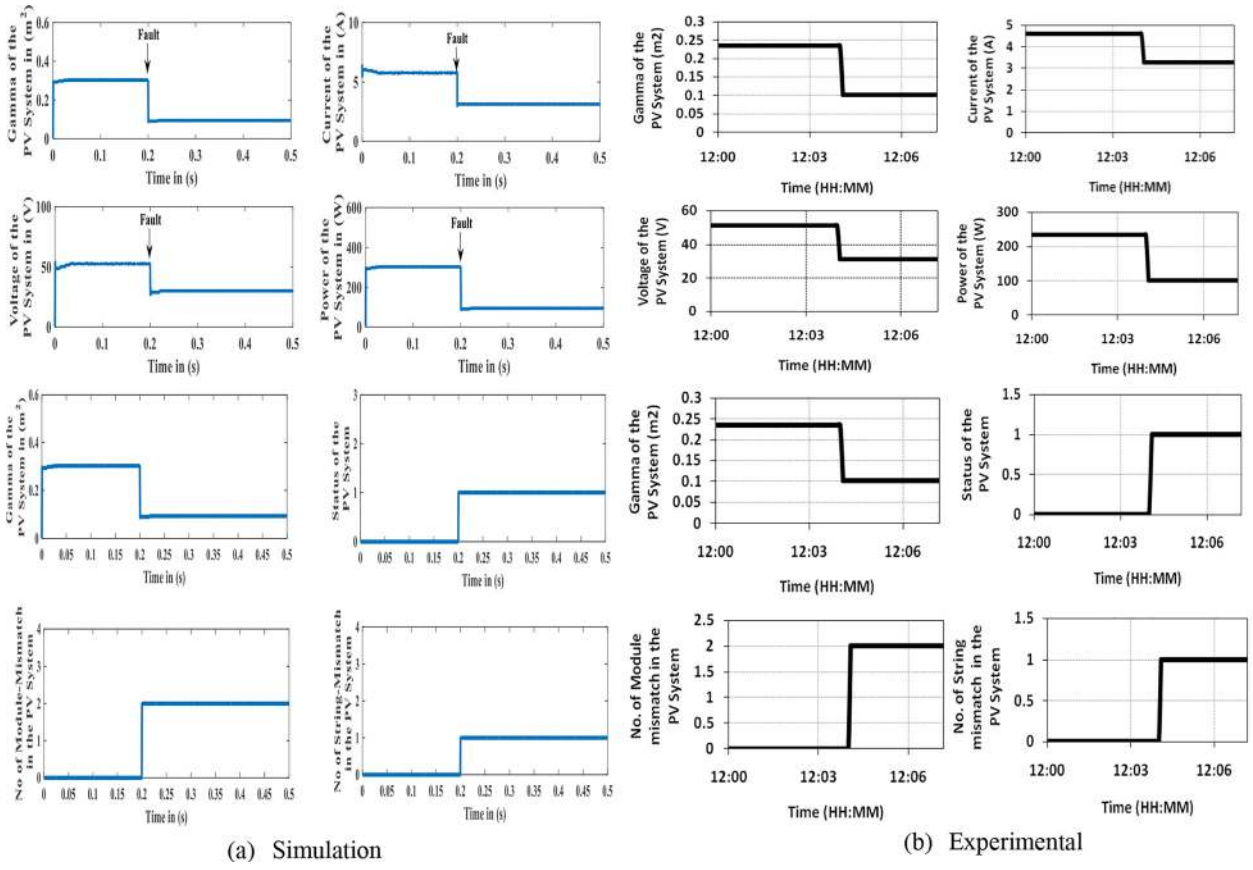

Figure 11: LL fault with two module-mismatches and one string-mismatch.

The simulation and experimental results with the proposed fault detection method for LL fault with one module mismatch and two string mismatches are as shown in Figure 12. It is observed that at instant of fault, there is a sudden drop in y which is less than the threshold value of "ε_3". Hence, the status of the PV system has been observed with "1" in Figure 12. This indicates that LL fault has occurred in PV system. Then the proposed fault detection method gives the number of module-mismatches equals to "1" and the number of string-mismatches equals to "2" as shown in Figure 12.

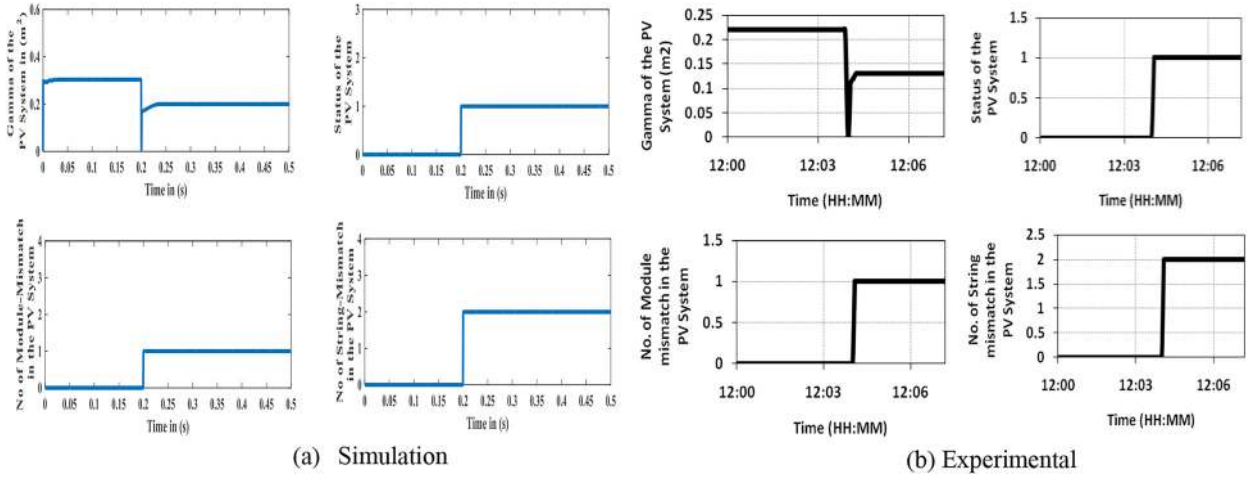

Figure 12: LL fault with one module-mismatch and two string-mismatches.

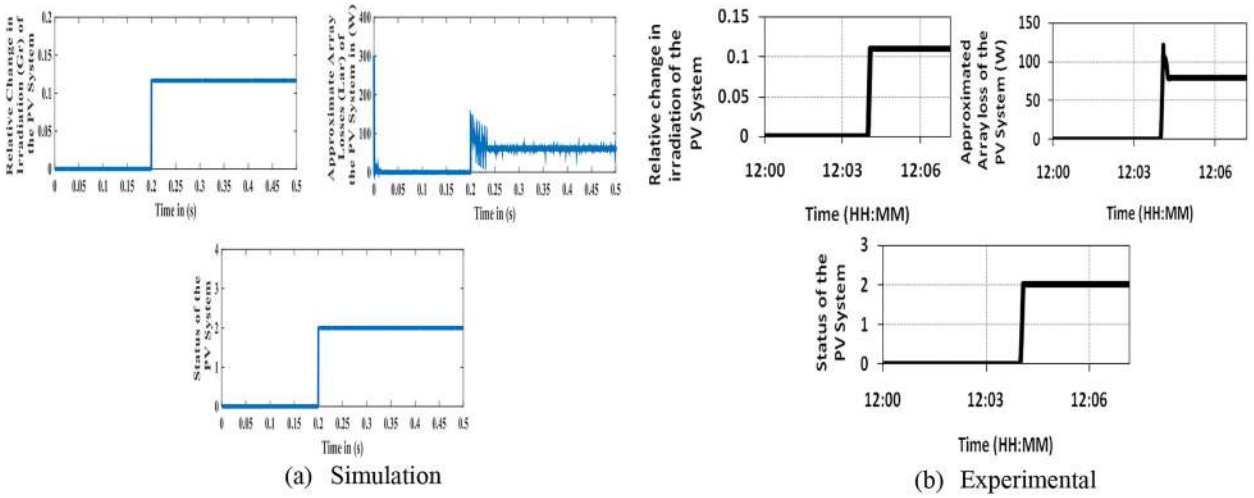

Figure 13: Partial shaded condition.

Case 4: Partial shaded condition (PSC).

The simulation and experimental results with the proposed fault detection method for PSC are as shown in Figure 13. It is observed that initially the value of Lar rises then it drops down to zero and the G_r maintains a constant value of zero till partial shade occurs. When partial shade occurs at 0.2 s in simulation and at 12 h 04 min in experimentation, there is a rise in both the value of G_r and Lar, which are more than the threshold value of εr_1 and εr_2 respectively as shown in Figure 13. This implies that the partial shade condition has occurred in PV system. Hence, the proposed method to detect faults in PV system has been differentiated the PSC and LL fault in PV system. Therefore the PV system status has been observed with "2" in Figure 13.

7 Conclusions

The proposed method with a systematic approach had successfully detected and differentiated the faults and partially shaded conditions by providing the status with type of the fault. Further, it also found the number of mismatch modules (or short-circuited bypass diodes) and mismatches strings (or open-circuited blocking diodes) under various mismatches conditions in Grid-connected PV system for dynamic change in irradiation. It can be easily incorporated in existing PV systems with conventional algorithms for MPPT such as P&O method without additional sensors, significant data, and hardware equipment. The theoretical performance had been validated with MATLAB/simulink simulations and small scale grid-connected PV systems developed in the laboratory. The results demonstrate the importance of the proposed algorithm by finding the number of mismatch modules (or short-circuited bypass diodes) and mismatch strings in grid-connected PV system. The proposed concept with experimental validation helps us to extend our work in future to find out the location of the faults/mismatch modules and strings in the large scale PV system.

Acknowledgment: The authors thank DST, India for granting project titled "Design and Development of Solar Photo-Voltaic Powered Cold Storage System" - Initiative to Promote Habitat Energy Efficiency (I-PHEE), and National Institute of Technology, Trichy, India, and Rajiv Gandhi University of Knowledge technologies, Basara, India, for providing facilities to carry out this work and Prof. S. Shravan Kumar, English Department at Rajiv Gandhi University of Knowledge technologies, Basara, India, for his suggestions in preparing this paper.

Author contribution: All the authors have accepted responsibility for the entire content of this submitted manuscript and approved submission.

Research funding: None declared.

Conflict of interest statement: The authors declare no conflicts of interest regarding this article.

References

1. Roman E, Alonso R, Ibanez P, Elorduizapatarietxe S, Goitia D. Intelligent PV module for grid-connected PV systems. IEEE Trans Ind Electron 2006;53:1066–73.
2. Hussain I, Kandpal M, Singh B. Grid integration of single stage solar PV system using three-level voltage source converter. DE GRUYTER Int J Emerging Electric Power Sys 2016;17:425–34.

3. Eltawil MA, Zhao Z. Grid-connected photovoltaic power systems: technical and potential problems—a review. ELSEVIER J Renew Sust Energy Rev 2010;14:112–29.
4. Madeti SR, Singh SN. A comprehensive study on different types of faults and detection techniques for solar photovoltaic system. ELSEVIER J Solar Energy 2017;158:161–85.
5. Zhao Y, De Palma JF, Mosesian J, Lyons R, Lehman B. Line–line fault analysis and protection challenges in solar photovoltaic arrays. IEEE Trans Ind Electron 2013;60:3784–95.
6. Alam MK, Khan F, Johnson J, Flicker J. A comprehensive review of catastrophic faults in PV arrays: types, detection, and mitigation techniques. IEEE J Photovolt 2015;5:982–97.
7. Zhao Y, Lehman B, De Palma JF, Mosesian J, Lyons R. Challenges to over current protection devices under line-line faults in solar photovoltaic arrays. Phoenix, AZ, USA: Energy Conversion Congress and Exposition (ECCE); 2011.
8. Zhao Y, Lehman B, Ball R, Mosesian J, De Palma JF. Outlier detection rules for fault detection in solar photovoltaic arrays. In: 28th annual IEEE applied power electronics conference and exposition (APEC). Long Beach, CA, USA; 2013.
9. Zhao Y, Balboni F, Arnaud T, Mosesian J, Ball R, Lehman B. Fault experiments in a commercial-scale PV laboratory and fault detection using local outlier factor. In: IEEE 40th Photovoltaic Specialist Conference (PVSC). IEEE, USA; 2014.
10. Jain P, Poon J, Singh JP, Spanos C, Sanders SR, Panda SKA. Digital twin approach for fault diagnosis in distributed photovoltaic systems. IEEE Trans Power Electron 2020;35:940–56.
11. Zhao Y, Saleh KA, Hooshyar A, El-Saadany EF, Zeineldin HH. Voltage-based protection scheme for faults within utility-scale photovoltaic arrays. IEEE Trans Smart Grid 2018;9: 4367–82.
12. Murtaza AF, Bilal M, Ahmad R, Sher HA. A circuit analysis based fault finding algorithm for photovoltaic array under LL/LG faults. IEEE J Emerg Select Topic Power Electron 2019:1, https://doi.org/10.1109/jestpe.2019.2904656.
13. Zhao Y, Ball R, Mosesian J, De Palma JF, Lehman B. Graph-based semi-supervised learning for fault detection and classification in solar photovoltaic arrays. IEEE Trans Power Electron 2015;30: 2848–58.
14. Akram MN, Lotfifard S. Modeling and health monitoring of DC side of photovoltaic array. IEEE Trans Sust Energy 2015;6:1245–53.
15. Chine W, Mellit A, Pavan AM, Kalogirou SA. Fault detection method for grid-connected photovoltaic plants. ELSEVIER J Renew Energy 2014;66:99–110.
16. Platon R, Martel J, Woodruff N, Chau TY. Online fault detection in PV systems. IEEE Trans Sust Energy 2015;6:1200–7.
17. Hu Y, Zhang J, Cao W, Wu J, Tian GY, Finney SJ, et al. Online two-section PV array fault diagnosis with optimized voltage sensor locations. IEEE Trans Ind Electron 2015;62:7237–46.
18. Hariharan R, Chakkarapani M, Saravanallango G, Nagamani CA. Method to detect photovoltaic array faults and partial shading in PV systems. IEEE J Photovolt 2016;6:1278–85.
19. Garoudja E, Harrou F, Sun Y, Kara K, Chouder A, Silvestre S. Statistical fault detection in photovoltaic systems. ELSEVIER J Solar Energy 2017;150:485–99.
20. Dhimish M, Holmes V, Mehrdadi B, Dales M. Multi-layer photovoltaic fault detection algorithm. IET J High volt 2017;2:244–52.
21. Yi Z, Etemadi AH. Fault detection for photovoltaic systems based on multi-resolution signal decomposition and fuzzy inference systems. IEEE Trans Smart Grid 2017;8:1274–83.
22. Chen L, Li S, Wang X. Quickest fault detection in photovoltaic systems. IEEE Trans Smart Grid 2018;9:1835–47.
23. Kumar BP, Ilango GS, Reddy MJB, Chilakapati N. Online fault detection and diagnosis in photovoltaic systems using wavelet packets. IEEE J Photovolt 2018;8:257–65.
24. Roy S, Alam MK, Khan F, Johnson J, Flicker J. An irradiance-independent, robust ground-fault detection scheme for PV arrays based on spread spectrum time-domain reflectometry (SSTDR). IEEE Trans Power Electron 2018;33:7046–57.
25. Pillai DS, Rajasekar N. An MPPT based sensorless line-line and line-ground fault detection technique for PV systems. IEEE Trans Power Electron 2018;34:8646–59.
26. Pillai DS, Blaabjerg F, Rajasekar N. A comparative evaluation of advanced fault detection approaches for PV systems. IEEE J Photovolt 2019;9:513–27.
27. Villalva MG, Gazoli JR, Ruppert Filho E. Comprehensive approach to modeling and simulation of photovoltaic arrays. IEEE Trans Power Electron 2009;24:1198–208.